Bio-Inspired Direct Patterning Functional Nanothin Microlines: Controllable Liquid Transfer

Qianbin Wang,[†] Qingan Meng,[†] Pengwei Wang,[†] Huan Liu,[*,†] and Lei Jiang[†,‡]

[†]Key Laboratory of Bio-Inspired Smart Interfacial Science and Technology of Ministry of Education, Beijing Key Laboratory of Bio-Inspired Energy Materials and Devices, School of Chemistry and Environment, Beihang University, Beijing 100191, People's Republic of China and [‡]Beijing National Laboratory for Molecular Sciences (BNLMS), Key Laboratory of Organic Solids, Institute of Chemistry, Chinese Academy of Sciences, Beijing 100190, People's Republic of China

ABSTRACT Developing a general and low-cost strategy that enables direct patterning of microlines with nanometer thickness from versatile liquid-phase functional materials and precise positioning of them on various substrates remains a challenge. Herein, with inspiration from the oriental wisdom to control ink transfer by Chinese brushes, we developed a facile and general writing strategy to directly pattern various functional microlines with homogeneous distribution and nanometer-scale thickness. It is demonstrated that the width and thickness of the microlines could be well-controlled by tuning the writing method, providing guidance for the adaptation of this technique to various systems. It is also shown that various functional liquid-phase materials, such as quantum dots, small molecules, polymers, and suspensions of nanoparticles, could directly write on the substrates with intrinsic physicochemical properties well-preserved. Moreover, this technique enabled direct patterning of liquid-phase materials on certain microdomains, even in multiple layered style, thus a microdomain localized chemical reaction and the patterned surface chemical modification were enabled. This bio-inspired direct writing device will shed light on the template-free printing of various functional micropatterns, as well as the integrated functional microdevices.

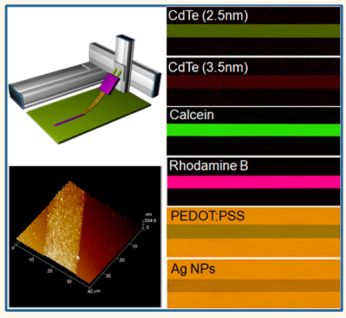

KEYWORDS: bio-inspired · microlines · nanothin · direct writing

Direct development of one-dimensional micropatterns as microlines and microstripes on certain substrates from various functional organic/inorganic liquid-phase materials has currently aroused intensive research interests due to their promising applications in versatile fields as integrated electric and optical microdevices, biosensors, and biodetection, where the device performance is heavily dependent on the dimension of the patterned functional materials.[1−3] It has been reported that miniaturization of organic/inorganic patterns down to the micrometer scale could significantly increase either the sensitivity in biological detection or the efficiency of biological diagnosis.[4,5] For example, the protein microarray with a typical nanostructure could dramatically enhance its near-infrared fluorescence property 100-fold and, therefore, was used in early detection of cancer biomarkers.[5] Moreover, micropatterned organic molecules, especially those with nanometer-scale thickness, could drastically improve the balance of electron and hole transfer and, therefore, improve the efficiency of the integrated semiconductor/optoelectronic device.[6−8] In this regard, we recently revealed that the well-defined polymer microwire arrays on certain substrates could lead to high-quality organic field-effect transistors, which was mainly attributable to the microscale confinement of the polymer.[9] Thus, various strategies have been developed to generate such one-dimensional micropatterns in the last several decades, such as photolithography,[10] microcontact printing,[11] and inkjet printing.[12] For example, photolithography was introduced to fabricate grids with line widths on the order of micrometers;[9,13,14] microcontact printing developed by Whitesides and co-workers was widely employed for direct fabrication of arrays at the micrometer and millimeter scale;[11,15,16] inkjet printing can be used to propel ink droplets onto paper, plastic, or other substrates in a predetermined pattern with a general resolution of hundreds of micrometers.[12,17−20] These methods are either costly or time-consuming, where normally

* Address correspondence to liuh@buaa.edu.cn.

Received for review February 6, 2015 and accepted April 6, 2015.

Published online April 06, 2015
10.1021/acsnano.5b00861

the complicated prepatterning process was necessary and also suffered from the common lack of flexibility in making patterns (*i.e.*, normally the duplicated transfer of the predesigned patterns onto the substrate). In addition, due to the technique limitation, it is rather difficult to downsize the patterns to nanometer scale in one dimension by using these methods. Therefore, developing a low-cost, template-free, yet efficient strategy to generate micropatterns directly on versatile substrates, especially those with nanometer scale in one dimension, is of paramount importance but is poorly developed.

Recently, Lewis and co-workers developed a pen-on-paper approach to provide a low-cost and template-free fabrication route for printing flexible electronic devices from certain silver nanoparticle-based ink (viscosity from ~0.3 to ~100 Pa·s).[21] However, this method suffered from both limitations of low resolution (several hundred micrometers to millimeters) of the as-written microlines and strict requirement on viscosity and coagulation behavior for the printed materials. So far, developing a general strategy that enabled direct patterning of microlines with nanometer thickness from versatile liquid-phase functional materials and precise positioning them on various substrates remains a challenge. Very recently, we revealed that the freshly emergent hairs (FE-hairs) enable the elaborate manipulation of low-viscosity liquid of silicon oil (viscosity = 5 mPa·s) and ink drop (viscosity = 9 mPa·s). With this advantage, the liquid material could be directly transferred onto the substrates of glass, silicon wafer, and paper homogeneously as an single microline and its patterns with a resolution down to 10 μm.[22] Herein, drawn from inspiration, we developed a facile and general FE-hairs-based strategy that enables direct patterning of various liquid-phase materials into functional microlines with controllable nanometer-scale thickness.

Noteworthy, by introducing 0.1 wt % poly(vinyl alcohol) (PVA) to modulate the surface energy and viscosity of the liquid materials,[23] the strategy is applicable to versatile liquid-phase materials such as quantum dots, fluorescence molecules, conductive polymers, and nanoparticle suspensions, which is of paramount importance for practical applications. Moreover, we demonstrated that the width and thickness of the as-generated microlines could be well-controlled by tuning the writing method (speed, direction, and pressure) by performing a series quantitative experiments, which provides guidance for the adaptation of this technique to various practical applications. We further demonstrated that this strategy is applicable for direct writing of various microline-based functional surfaces, including electrically conductive or fluorescent microlines, localized chemical reactions, and surface chemical modifications in microdomains. We envision that this bio-inspired direct writing device will shed new light on developing the novel template-free printing strategies for easy printing of various functional micropatterns, as well as the integrated functional microdevices.

RESULTS AND DISCUSSION

The model of the as-developed writing device is schematically shown in Figure 1a, which contains three main components of the writing unit, liquid supply unit, and motion control unit. Specifically, the writing unit consisted of two FE-hairs arranged vertically in parallel to each other with the top end clamped and the bottom end free to move and was connected with an artificially made liquid reservoir for continuous liquid supply, serving as the liquid supply unit. A programmable three-axis (*x*-*y*-*z*) motion stage was used to control the motion velocity and direction of the writing device, as well as the interaction between the writing units and the substrates. Upon contact of the writing unit with the substrate of smooth paper, glass, or silicon wafer, the liquid materials stored in the writing device would be continuously and controllably transported downstream onto the substrate, driven by the cooperative forces of gravity, Laplace pressure difference, and asymmetrical retention force that were microstructure-dependent.[22,24,25] As a result, a durative microline could be successfully generated following the FE-hairs' moving direction, which was similar to the ink stroke by Chinese brushes.[22]

We first demonstrated that the bio-inspired writing device enables controllable liquid transfer onto certain substrates by using aqueous ink with a surface tension of 45 mN/m. Scanning electron microscopy (SEM) was used to characterize the microstructure of the as-prepared ink microline on smooth glass, and the SEM images illustrated its well-defined profile. As given in Figure 1b, a long microline with a diameter of ~50 μm exhibits a constant width along the whole long ink stroke. Magnified images (Figure 1c) revealed that the boundary of the ink microline was very regular. Only nanoscaled fluctuations were observed in a few places. Moreover, the distribution of ink particles was uniform in the whole microline (Figure 1d). The well-defined profile and the uniformity of the as-generated microline could be further evidenced by the atomic force microscopy (AFM) measurement, where fluctuation was detected within the whole microline with only several tens of nanometers (Supporting Information Figure S1). More importantly, the as-generated microline had a thickness of about 100 nm (Figure 1e−g), which could be further controlled within the range of 42 to 141 nm (Figure 2c). These results clearly showed that the as-developed strategy appears to be an effective approach to directly write nanothin microlines with a well-defined profile and uniform distribution.

The main feature of this direct writing technique is the flexibility and controllability: by accurately tuning the method of writing device motion (moving speed,

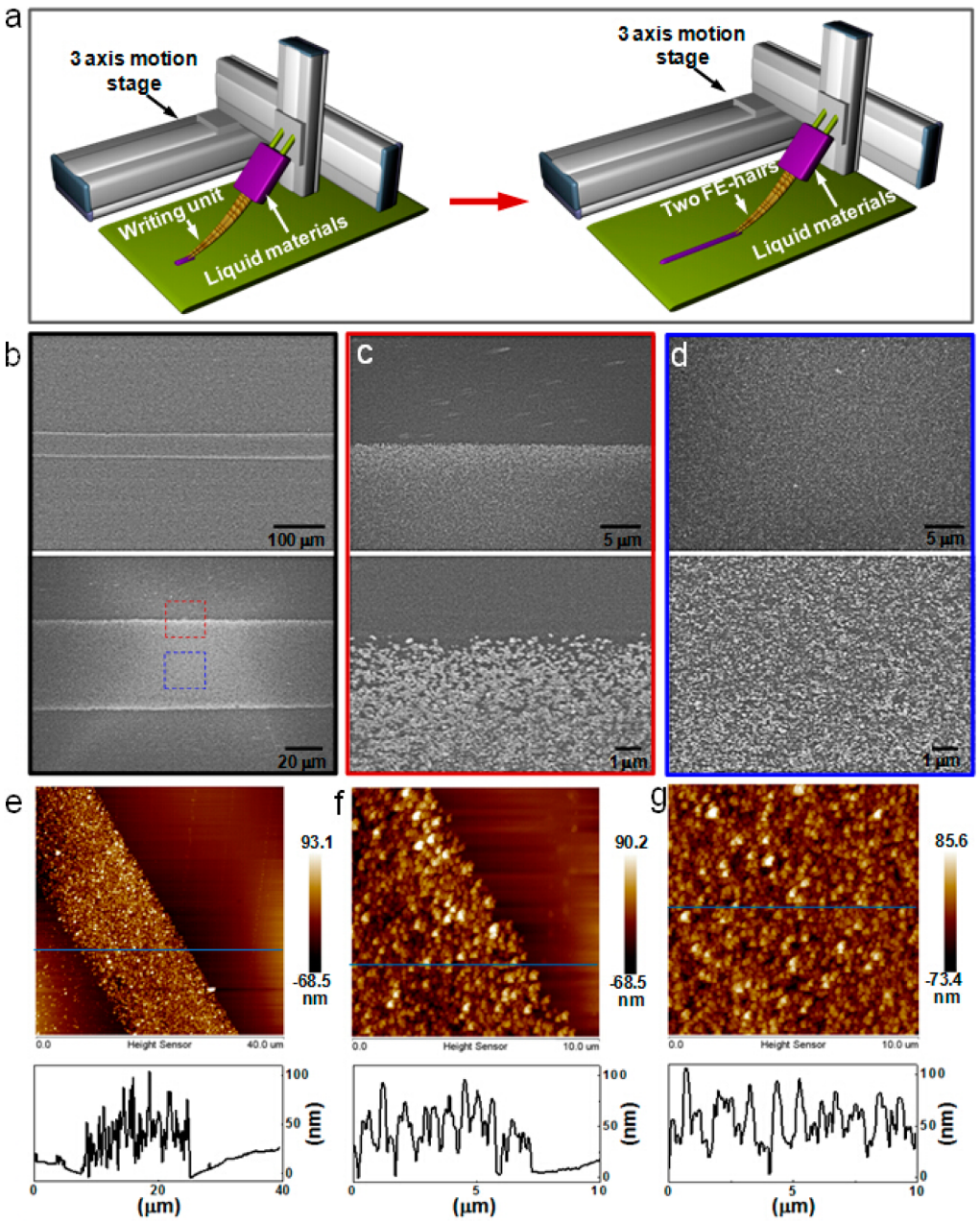

Figure 1. Direct patterning nanothin microlines by a bio-inspired direct writing device. (a) Schematic illustration of the bio-inspired direct writing device where two parallel FE-hairs were connected with an artificially made liquid reservoir for continuous liquid supply, and a programmable three-axis (*x*-*y*-*z*) motion stage was used to accurately control the motion velocity and direction of the substrate. (b–d) SEM images of the as-prepared ink microline. By using a bio-inspired direct writing device, ink nanothin microline with a constant width could be successfully obtained (b). The boundary of the nanothin microline is rather regular with only a few nanoscale fluctuations (c). Magnified images reveal that the ink particles were homogeneously distributed throughout the whole microline (d). (e–g) AFM images of the as-prepared ink nanothin microline: the microline exhibits homogeneous distribution within all of the printing area with a thickness of about 100 nm.

direction, and area) and the surface tension and viscosity of the liquid material by introducing 0.1 wt % PVA, the microline patterns as well as its physicochemical properties can be well-controlled. For the direct writing process, the fluid is carried out within a narrow gap between the FE-hairs by a moving the printing device, as sketched in Figure 2a. The printed nanothin microlines are uniform when the flow is steady and two-dimensional. When the flow in the tip of the device was described by the complete two-dimensional, steady-state mass and momentum conservation equations coupled with an algebraic constitutive equation that approximates the non-Newtonian behavior of the liquid, the thickness of the printed microlines can be expressed as[26]

$$T = \frac{q}{U}$$

where q is the liquid flow rate per unit width and U is the speed of the moving printing device. The thickness of

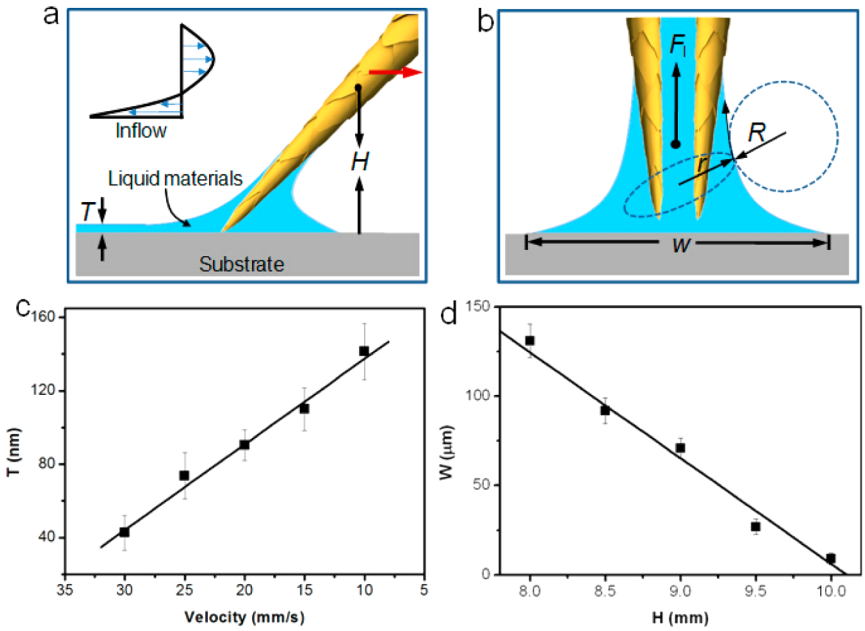

Figure 2. Mechanism and controllable writing of nanothin microlines. (a) Liquid flowing on the substrate could be affected by the motion stage, which would determine the width (*W*) and thickness (*T*) of the microlines. (b) Remarkable conicity at the tip of the FE-hairs would generate a Laplace pressure difference force to act on the liquid materials, which would contribute to the controllable ink transfer process. (c) Change in the velocity (*V*) of the substrate can significantly affect the thickness (*T*) of the microlines, and *V* is linearly inversely proportional to *T*. (d) By controlling the height of a fixed reference point on the FE-hair to the substrate (*H*), microlines with different widths could be generated, and *H* is positive in correlation with *W*.

the printed microline depends on the writing speed, lip lengths, gap shape, liquid surface tension, and rheology.

Another possible mechanism to control the ink transfer process arises from the conical structure of the FE-hairs, which will generate a difference in Laplace pressure.[22,24,27] When liquid flows at the tip of the FE-hairs, the force of difference in Laplace pressure, F_l, that can be obtained by integrating the Laplace pressure difference (ΔP) times the area around the entire liquid surface[27,28] can be expressed as $F_l \sim 2\int\pi(x - r_{hair})^2 d\Delta P$, where r_{hair} is the radius of the FE-hairs and ΔP is given by the Young−Laplace equation: $\Delta P \sim \gamma(1/r + 1/R)$ (r and R are orthogonal radii of curvature of the liquid as indicated in Figure 2b). The remarkable conicity at the tip of the FE-hairs could therefore generate a huge force that acts on the liquid materials, which would help to balance the liquid within the FE-hairs. In other words, F_l is a force that acts as a resistance for the liquid flowing out of the FE-hairs and consequently confines the flow *via* FE-hairs. The liquid materials slowly and continuously transfer onto the substrate in a controllable manner mainly under the cooperative force of conical tip-induced Laplace pressure difference and gravity.

To better understand the mechanism of the direct writing procedure, we evaluated the effect of different writing styles on the parameters of the as-generated nanothin microlines. It is found that the motion velocity (*V*) could significantly influence the thickness (*T*) of the printed microlines accurately, and *V* was linearly inversely proportional to *T*, as shown in Figure 2c. For a small motion velocity ($V = 10$ mm/s), the liquid material has enough time to transfer onto the substrate, resulting in a relatively thick microline on the glass surface ($T = 141$ nm). For a large velocity ($V = 30$ mm/s), the force-limited liquid materials could not be sufficiently flowed onto the surface of the substrate. Consequently, we obtained a much thinner microline on the glass ($T = 42$ nm). Similarly, we evaluated the effect of *H*, which is the height of a fixed reference point on the FE-hair to the substrate, on the width (*W*) of the microlines. The result indicated that the *H* presented a negative correlation with *W*, as illustrated in Figure 2d and Figure S2. We considered that the *H* is related to the contact area between the FE-hairs and the substrate, which would contribute to the width of the printed microlines. Generally, by varying the physical parameters of the writing device, liquid materials could be directly printed onto the substrate with a controllable width and thickness, presenting a well-controlled manner.

Developing an adaptation of this technique to generate various functional nanothin microlines using different liquid-phase materials, including functional small-molecules/macromolecules and nanoparticles, will be a practical application. By introducing 0.1 wt % PVA to modulate the surface tension and viscosity of the liquid materials, we successfully expanded this direct printing technique to generate various functional nanothin microlines from versatile functional liquid-phase materials, such as quantum dots, fluorescent

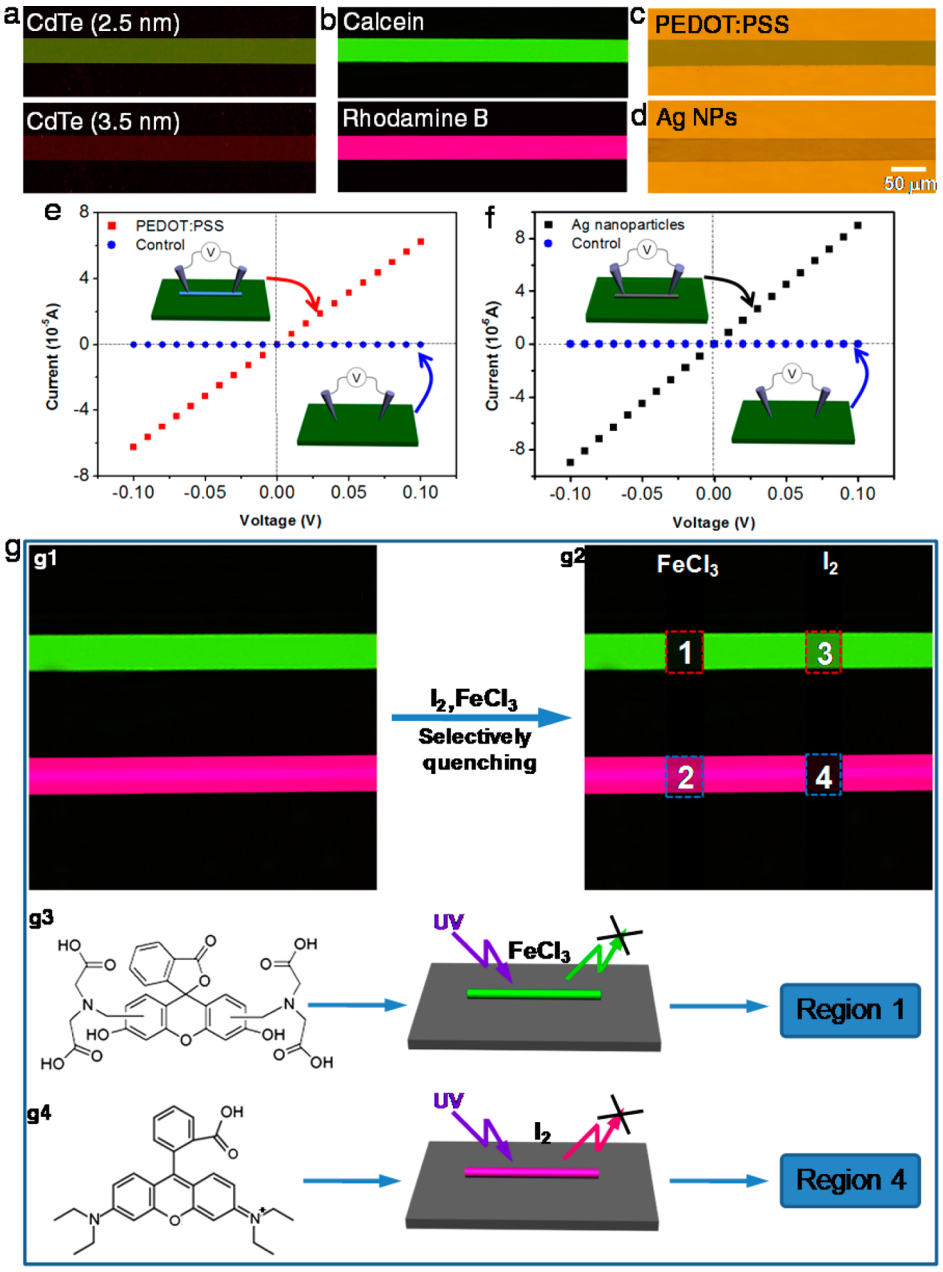

Figure 3. Direct writing of functional nanothin microlines and their applications. (a–d) Various functional liquid-phase materials, including (a) quantum dots (CdTe), (b) fluorescent molecules (calcein and rhodamine B), (c) conductive polymers (poly(3,4-ethylenedioxythiophene):poly(styrenesulfonate) (PEDOT:PSS), and (d) colloidal silver nanoparticles (AgNPs), could be directly written onto glass substrates with well-defined profiles and uniform distribution. (e,f) *I–V* behaviors of the PEDOT:PSS and AgNP microlines showed that the microlines could be endowed with conductive properties when conductive polymer (e) and AgNPs (f) were used as liquid materials. (g) Calcein and rhodamine B microlines could exhibit green and orange fluorescence under UV irradiation (g1). When exposed to $FeCl_3$ or I_2 solution, the fluorescence of the calcein and rhodamine B could be selectively quenched (g2) because the ferric compounds would react only with calcein molecules (g3), while the iodine molecule would selectively react with rhodamine B (g4).

small molecules, conductive polymers, and colloidal silver nanoparticle (AgNP) solution on diverse substrates (including flat surfaces of paper, glass, silicon wafer, plastics, and composite materials), as shown in Figure 3a–d. The well-defined profile and homogeneous thickness of the microlines could be confirmed by the uniform fluorescence intensity throughout the whole microline. Significantly, it is found that the physicochemical properties of the printed nanothin microlines were well-reserved: CdTe quantum dots with diameters of 2.5 and 3.5 nm are green and red, respectively (Figure 3a);[29,30] the calcein microline could exhibit green fluorescence when exposed at UV light, and the rhodamine B exhibits red fluorescence (Figure 3b). We consider that the as-printed functional nanothin microlines might be scientifically meaningful for fields of optical/electronic devices, bio/chemical sensors, and other nanotechnology.[25]

The ability to directly write functional microlines enables exploration of the application of microscaled circuits. To effectively deliver electrons through the microlines, poly(3,4-ethylenedioxythiophene): poly(styrenesulfonate) (PEDOT:PSS, with 0.8 wt % PEDOT and 0.5 wt % PSS) solution (5 wt % in water with addition of 5 wt % dimethyl sulfoxide to enhance the conductivity) was used as the liquid material to generate conductive microlines by the direct writing device. Here, the *I*−*V* curve was taken to characterize the conductivity of the PEDOT:PSS microlines. The result shows that a 50 μm wide PEDOT:PSS microline could carry a current of 62.4 μA at 0.1 V impressed voltage. As a control, the *I*−*V* curve for a naked glass surface was measured (Figure 3e, blue line), and no electric conductivity was observed. Similarly, the *I*−*V* behaviors for the AgNP microline presented the reasonable electronic property, suggesting its potential application in microscaled circuits (Figure 3f). Given these facts, it can be concluded that the as-developed strategy enables direct writing of single functional microlines with uniform distribution and a well-defined profile, where the intrinsic physicochemical property could be well-preserved or even enlarged.

Furthermore, by virtue of the nanometer-scale thickness of the as-written microlines, multiple layered cross connections were enabled, where the reaction could be strictly localized in certain microdomains. Here, we demonstrated that this direct writing strategy enables the generation of multiple different functional microlines, even with multiple layered cross connections, on certain substrates using the programmable three-dimensional mobile stage, which may find promising applications in low-cost, turn-on chemosensors.[31,32] It is well-known that calcein is an excellent candidate for metallic ion sensors because it exhibits green fluorescence under UV light and quenches when in contact with metallic salts (Figure S3),[33] while rhodamine B would lose its fluorescence when reacting with iodine (I_2).[34] Specifically, we directly wrote calcein and rhodamine B microlines and then employed this microline-based surface as an analytical sensing device, as presented in Figure 3g. First, calcein and rhodamine B microlines were directly written on a flat glass substrate and located parallel to each other. Under UV irradiation, the calcein and rhodamine B microlines exhibited homogeneous green and orange fluorescence due to the uniform distribution of the fluorescence molecule (Figure 3g1). Then we printed another ferric chloride ($FeCl_3$) microline that was vertically across the prewritten calcein and rhodamine B microlines, as illustrated in Figure 3g2. When the calcein and rhodamine B microlines wereexposed to $FeCl_3$ for several minutes, the fluorescence of the crosspoint microdomain of the calcein and $FeCl_3$ microlines (region 1) was quenched, while the color of region 2 remains orange because the ferric compounds would only react with calcein molecules (Figure 3g3), indicating a novel fluorimetric detection of ferric compounds. Similarly, an I_2 microline was directly written vertically across the calcein and rhodamine B nanothin microlines, and as a result, only the fluorescence of the microdomain where the rhodamine B microline overlapped with I_2 microline was quenched. Since the iodine molecule would selectively react with rhodamine B, the common domain of the rhodamine B microline (region 4) would lose its orange fluorescence and become dark, while the green one (calcein) survives (region 3), indicating a selective quenching reaction that occurs on the microlines. Therefore, this nanothin microline-based device showed a selective detection of diverse target compounds, which might find some applications in optical and sensing fields.

Associated with a programmable three-axis (*x*-*y*-*z*) motion stage, our direct writing device enables one to generate programmed nanothin microline arrays, which allows surface chemical modification at selective microdomains (Figure 4a) and consequently leads to a surface with designed wettability. Here, a fluoroalkylsilane (FAS)-modified glass was used as the substrate, and the hydrophilic silicon dioxide nanoparticles (SiO_2 NPs) with 0.1 wt % PVA solution was used as the liquid materials to generate a surface with an anisotropic wetting behavior. The water contact angle (CA) of the FAS-modified glass was measured to be 114° (inset in Figure 4a), exhibiting hydrophobicity, while the intrinsic water CA of SiO_2 NPs/PVA was ∼15° (Figure S4), a typical hydrophilic nature. By moving the writing device in a programmable way, an array of SiO_2 NP microlines was successfully generated on the FAS glass with a uniform width of 112 μm and the interspace of 103 μm (Figure 4b,c). The optical image of the SiO_2 NP microlines demonstrated their well-defined boundary with no obvious detectable fluctuations, and the dark and bright areas correspond to the SiO_2 NP microlines and the glass substrate, respectively (Figure 4b). Magnified SEM images reveal that the nanothin microlines consisted of uniform and dense SiO_2 nanoparticles with diameters of ∼70 nm, as presented in Figure 4d. Typical anisotropic wetting behavior was observed when a droplet of deionized water was gently placed on the microline-patterned surface (Figure 4e). As shown in Figure 4e, the contact line (CL) of the water droplet *via* the direction parallel with the microlines (*x*-axis direction) showed a steady increase with increasing time from 0 min to 3−6 min (front view), while the contact line *via* the direction perpendicular to the microlines (*y*-axis direction) remains unchanged with the increase of time (side view), indicating the typical anisotropic wetting behavior of this nanothin microline-patterned surface. This is because the vapor−liquid−solid (V−L−S) three-phase contact line (TCL) is continuous along the parallel direction of the microlines (*x*-axis direction) and discontinuous toward

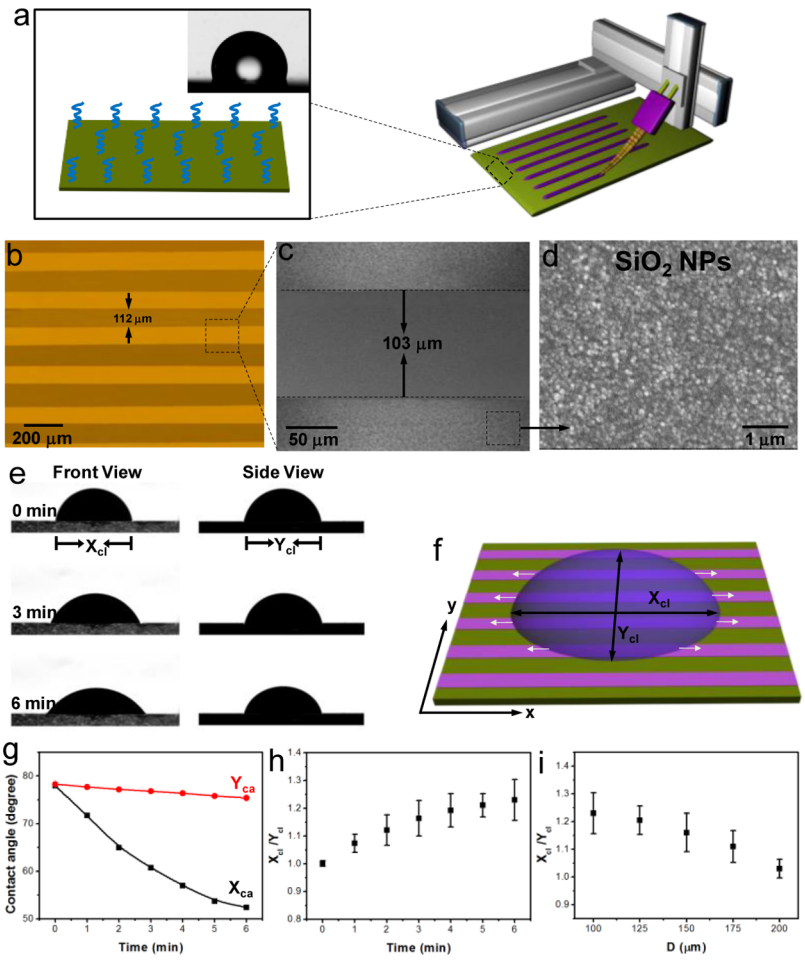

Figure 4. Direct writing line-patterned surface with parallel microline arrays and its application in anisotropic wetting. (a) Schematic illustration of a microline array direct writing device, where a programmable three-dimensional mobile stage was used to control the motion. (b–d) Optical and SEM images indicated that regular microlines were arranged in parallel with a distance of ~100 μm, and the SiO_2 nanoparticles were uniformly distributed throughout the whole microline. (e) Typical anisotropic spreading behavior of a pure water droplet on the microline-patterned surface indicated that the contact line along the *x*-axis direction showed a steady increase, while the contact line along the *y*-axis direction remained unchanged with the increase of time. (f) When a drop of water was placed on the microline-patterned surface, anisotropic spreading could take place since the vapor–liquid–solid three-phase contact line is continuous along the *x*-axis direction and discontinuous toward the *y*-axis direction. (g) Change of contact angles in different directions indicated the anisotropic wetting behavior of the droplet. (h) Droplet distortion (X_{CL}/Y_{CL}) as time increases demonstrated that the spreading in the *x*-axis direction is easier than that in the *y*-axis direction. (i) Change of distances (*D*) between the microlines could significantly affect the droplet anisotropic spreading behavior, and the droplet distortion became weaker with an increase of *D*.

the orthogonal direction (*y*-axis direction).[35] We monitored the changes of CAs and CLs as the drop spread and found that the CAs in the *x*-axis direction (X_{ca}) showed a quick decrease, while those in the orthogonal direction (Y_{ca}) were almost unchanged, as shown in Figure 4g. To better understand the anisotropic spreading of the droplet, we use "X_{CL}/Y_{CL}", that is, the ratio between two principal CLs in the parallel and orthogonal directions of the droplet, to evaluate the droplet distortion. As time increased from 0 to 6 min, the droplet was distorted more obviously because the spreading in the *x*-axis direction was easier than that in the *y*-axis direction (Figure 4h). Note that the anisotropic wetting behavior could be tuned by changing the distances (*D*) between the microlines, which could be easily realized by a programmable controlled writing device. As shown in Figure 4i, the distortion of the droplet on such a microline-patterned surface was weakened by increasing the *D*.

CONCLUSIONS

In conclusion, inspired by the controllable ink transfer of Chinese brushes, we developed a bio-inspired direct writing device which enabled direct writing of homogeneous nanothin microlines and their patterns on various substrates. Importantly, this strategy is applicable to various functional liquid-phase materials, including quantum dots, fluorescence molecules, conductive polymers, and suspensions of Ag and SiO_2 nanoparticles, exhibiting rather good generality. The parameters of the as-generated microlines (thickness, width, and distance within them) could be well-controlled by

tuning the writing style (velocity, moving direction, and pressure) flexibly. The as-prepared nanothin microlines could exhibit their intrinsic physicochemical properties or even enhanced performances due to the microscale confinement, which therefore leads to various functional microline-based devices as fluorescence and conductive microcircuits. Typically, by this technique, the chemical reaction could be well-confined at certain microdomains, which is applicable for chemical sensors and detection microdevices. Also, this technique enabled direct surface chemical modification on certain microdomains, leading to special wetting properties. We therefore anticipate that this bio-inspired direct writing device will shed light on the design of novel template-free printing devices and is applicable to various functional liquid-phase materials for easy printing of optical, electric, and sensing devices.

EXPERIMENTAL SECTION

Materials. The calcein and rhodamine B were purchased from Fluka. Ink was purchased from Beijing Jinghua Brush Co., Ltd. Silver nanoparticles (AgNPs) were prepared according to previous literature.[36] Quantum dots were kindly provided by Prof. Mingyuan Gao at ICCAS. Conductive PEDOT:PSS (5 wt %) was obtained from Sigma-Aldrich, and the solution was filtered through a 0.2 μm filter membrane before use. PVA (M_w = 85 000−124 000), $FeCl_3$, and I_2 were purchased from Sigma-Aldrich. The above chemical reagents were all used as received.

Experiments on the Template-Free Direct Writing Device. The template-free direct writing device was fabricated by using parallel FE-hairs which were fixed within a glass tube. Various liquid-phase solutions (ink, quantum dots, fluorescence molecules, conductive polymers, and silver nanoparticles with 0.1 wt % PVA) were poured into the glass tube for continuous liquid supply. For conductive nanoparticle ink, AgNP content was 5 wt %, the concentration of PEDOT:PSS was 5 wt % dispersion in water, and 5 wt % dimethyl sulfoxide was added to enhance the conductivity in the conductive polymer ink. The concentrations of calcein, rhodamine B, CdTe (2.5 nm), and CdTe (3.5 nm) used in our experiment were 100, 100, 9.67, and 13.8 mg/L, respectively. All experiments were performed at room temperature.

Characterization of the Microstructures. The optical images of the microlines were recorded by a digital video camera (WV-CP280/CH, Panasonic, Japan). The microstructures of the microlines were observed by a field-emission scanning electron microscope (JEOL, JSM-6700F, Japan) and an atomic force microscope (SPI 3800N, Japan).

Electrical Measurement for Conductive Microlines. The electrical measurement was characterized under ambient conditions using a Keilthley 4200-SCS semiconductor system and the Suss PM5 analytical probe station in a clean and shielded box in the dark. Two platinum conical probes were placed to contact with the site of PEDOT:PSS or the AgNP microline, and impressed voltage was applied to detect the corresponding current.

Sensing Device. Precisely printed calcein and rhodamine B microlines were generated upon the surface of a smooth glass. The mcirowire-based surface exhibited green and orange fluorescence under UV irradiation. When another perpendicular $FeCl_3$ or I_2 microline was printed, the fluorescence in the intersection region was selectively quenched, indicating a novel fluorimetric detection of Fe^{3+} and I_2.

Anisotropic Wetting. A 5 μL deionized water droplet was deposited on the directly written microline-patterned surface. The contact angle and contact line were recorded per minute by using a Dataphysics OCA20 contact angle measuring system at ambient temperature.

Conflict of Interest: The authors declare no competing financial interest.

Supporting Information Available: AFM images of ink microline; ink microlines with various widths; a ferric salt sensor based on the fluorescence quenching property of functional microlines; contact angle of SiO_2 NP/PVA film. This material is available free of charge *via* the Internet at http://pubs.acs.org.

Acknowledgment. The authors thank the National Research Fund for Fundamental Key Projects (2013CB933000), Program for New Century Excellent Talents in University (NCET-13-0024), National Natural Science Foundation (61227902, 21421061), the Key Research Program of the Chinese Academy of Sciences (KJZD-EW-M01), the 111 Project (No. B14009), and the Fundamental Research Funds for the Central Universities for financial support.

REFERENCES AND NOTES

1. Chen, Z.; Pan, D.; Li, Z.; Jiao, Z.; Wu, M.; Shek, C.-H.; Wu, C. L.; Lai, J. K. Recent Advances in Tin Dioxide Materials: Some Developments in Thin Films, Nanowires, and Nanorods. *Chem. Rev.* **2014**, *114*, 7442–7486.
2. Polla, D.; Francis, L. Ferroelectric Thin Films in Micro-electromechanical Systems Applications. *MRS Bull.* **1996**, *21*, 59–65.
3. Wen, Y.; Liu, Y. Recent Progress in N-Channel Organic Thin-Film Transistors. *Adv. Mater.* **2010**, *22*, 1331–1345.
4. Hu, W.; Liu, Y.; Yang, H.; Zhou, X.; Li, C. M. ZnO Nanorods-Enhanced Fluorescence for Sensitive Microarray Detection of Cancers in Serum without Additional Reporter-Amplification. *Biosens. Bioelectron.* **2011**, *26*, 3683–3687.
5. Tabakman, S. M.; Lau, L.; Robinson, J. T.; Price, J.; Sherlock, S. P.; Wang, H.; Zhang, B.; Chen, Z.; Tangsombatvisit, S.; Jarrell, J. A. Plasmonic Substrates for Multiplexed Protein Microarrays with Femtomolar Sensitivity and Broad Dynamic Range. *Nat. Commun.* **2011**, *2*, 466.
6. Botiz, I.; Darling, S. B. Optoelectronics Using Block Copolymers. *Mater. Today* **2010**, *13*, 42–51.
7. Han, T.-H.; Lee, Y.; Choi, M.-R.; Woo, S.-H.; Bae, S.-H.; Hong, B. H.; Ahn, J.-H.; Lee, T.-W. Extremely Efficient Flexible Organic Light-Emitting Diodes with Modified Graphene Anode. *Nat. Photonics* **2012**, *6*, 105–110.
8. Muccini, M. A Bright Future for Organic Field-Effect Transistors. *Nat. Mater.* **2006**, *5*, 605–613.
9. Wu, Y.; Su, B.; Jiang, L.; Heeger, A. J. "Liquid−Liquid−Solid"-Type Superoleophobic Surfaces To Pattern Polymeric Semiconductors towards High-Quality Organic Field-Effect Transistors. *Adv. Mater.* **2013**, *25*, 6526–6533.
10. Sun, Y.; Rogers, J. A. Fabricating Semiconductor Nano/Microwires and Transfer Printing Ordered Arrays of Them onto Plastic Substrates. *Nano Lett.* **2004**, *4*, 1953–1959.
11. Wilbur, J. L.; Kumar, A.; Kim, E.; Whitesides, G. M. Microfabrication by Microcontact Printing of Self-Assembled Monolayers. *Adv. Mater.* **1994**, *6*, 600–604.
12. Sirringhaus, H.; Kawase, T.; Friend, R.; Shimoda, T.; Inbasekaran, M.; Wu, W.; Woo, E. High-Resolution Inkjet Printing of All-Polymer Transistor Circuits. *Science* **2000**, *290*, 2123–2126.
13. Rogers, J. A.; Paul, K. E.; Jackman, R. J.; Whitesides, G. M. Using an Elastomeric Phase Mask for Sub-100 nm Photolithography in the Optical Near Field. *Appl. Phys. Lett.* **1997**, *70*, 2658–2660.
14. Levenson, M. D.; Viswanathan, N.; Simpson, R. A. Improving Resolution in Photolithography with a Phase-Shifting Mask. *IEEE Trans. Electron Devices* **1982**, *29*, 1828–1836.
15. Mrksich, M.; Whitesides, G. M. Patterning Self-Assembled Monolayers Using Microcontact Printing: A New Technology for Biosensors?. *Trends Biotechnol.* **1995**, *13*, 228–235.

16. Jackman, R. J.; Wilbur, J. L.; Whitesides, G. M. Fabrication of Submicrometer Features on Curved Substrates by Microcontact Printing. *Science* **1995**, *269*, 664–666.
17. Zhang, L.; Liu, H.; Zhao, Y.; Sun, X.; Wen, Y.; Guo, Y.; Gao, X.; Di, C. A.; Yu, G.; Liu, Y. Inkjet Printing High-Resolution, Large-Area Graphene Patterns by Coffee-Ring Lithography. *Adv. Mater.* **2012**, *24*, 436–440.
18. Derby, B. Inkjet Printing of Functional and Structural Materials: Fluid Property Requirements, Feature Stability, and Resolution. *Annu. Rev. Mater. Res.* **2010**, *40*, 395–414.
19. de Gans, B. J.; Duineveld, P. C.; Schubert, U. S. Inkjet Printing of Polymers: State of the Art and Future Developments. *Adv. Mater.* **2004**, *16*, 203–213.
20. Calvert, P. Inkjet Printing for Materials and Devices. *Chem. Mater.* **2001**, *13*, 3299–3305.
21. Russo, A.; Ahn, B. Y.; Adams, J. J.; Duoss, E. B.; Bernhard, J. T.; Lewis, J. A. Pen-on-Paper Flexible Electronics. *Adv. Mater.* **2011**, *23*, 3426–3430.
22. Wang, Q.; Su, B.; Liu, H.; Jiang, L. Chinese Brushes: Controllable Liquid Transfer in Ratchet Conical Hairs. *Adv. Mater.* **2014**, *26*, 4889–4894.
23. Tang, Y.; Gong, S.; Chen, Y.; Yap, L. W.; Cheng, W. Manufacturable Conducting Rubber Ambers and Stretchable Conductors from Copper Nanowire Aerogel Monoliths. *ACS Nano* **2014**, *8*, 5707–5714.
24. Wang, Q.; Meng, Q.; Chen, M.; Liu, H.; Jiang, L. Bio-Inspired Multistructured Conical Copper Wires for Highly Efficient Liquid Manipulation. *ACS Nano* **2014**, *8*, 8757–8764.
25. Wang, Q.; Meng, Q.; Liu, H.; Jiang, L. Chinese Brushes: From Controllable Liquid Manipulation to Template-Free Printing Microlines. *Nano Res.* **2015**, *8*, 97–105.
26. Romero, O.; Suszynski, W.; Scriven, L.; Carvalho, M. Low-Flow Limit in Slot Coating of Dilute Solutions of High Molecular Weight Polymer. *J. Non-Newtonian Fluid Mech.* **2004**, *118*, 137–156.
27. Lorenceau, É.; Quéré, D. Drops on a Conical Wire. *J. Fluid Mech.* **2004**, *510*, 29–45.
28. Zheng, Y.; Bai, H.; Huang, Z.; Tian, X.; Nie, F.-Q.; Zhao, Y.; Zhai, J.; Jiang, L. Directional Water Collection on Wetted Spider Silk. *Nature* **2010**, *463*, 640–643.
29. Li, Y.; Jing, L.; Qiao, R.; Gao, M. Aqueous Synthesis of CdTe Nanocrystals: Progresses and Perspectives. *Chem. Commun.* **2011**, *47*, 9293–9311.
30. Gao, M.; Sun, J.; Dulkeith, E.; Gaponik, N.; Lemmer, U.; Feldmann, J. Lateral Patterning of CdTe Nanocrystal Films by the Electric Field Directed Layer-by-Layer Assembly Method. *Langmuir* **2002**, *18*, 4098–4102.
31. Wu, Y.; Su, B.; Jiang, L. Smartly Aligning Nanowires by a Stretching Strategy and Their Application as Encoded Sensors. *ACS Nano* **2012**, *6*, 9005–9012.
32. Kim, H. N.; Guo, Z.; Zhu, W.; Yoon, J.; Tian, H. Recent Progress on Polymer-Based Fluorescent and Colorimetric Chemosensors. *Chem. Soc. Rev.* **2011**, *40*, 79–93.
33. Breuer, W.; Epsztejn, S.; Millgram, P.; Cabantchik, I. Z. Transport of Iron and Other Transition Metals into Cells as Revealed by a Fluorescent Probe. *Am. J. Physiol.* **1995**, *37*, C1354.
34. Milborrow, B. Iodine Quenched Fluorescence, a Sensitive, Non-destructive a Method for the Detection of Organic Compounds on Chromatoplates. *J. Chromatogr., A* **1965**, *19*, 194–197.
35. Yoshimitsu, Z.; Nakajima, A.; Watanabe, T.; Hashimoto, K. Effects of Surface Structure on the Hydrophobicity and Sliding Behavior of Water Droplets. *Langmuir* **2002**, *18*, 5818–5822.
36. TekaiaáElhsissen, K. Preparation of Colloidal Silver Dispersions by the Polyol Process. Part 1—Synthesis and Characterization. *J. Mater. Chem.* **1996**, *6*, 573–577.